BIOMOLECULES & THERAPEUTICS

Invited Review
Biomol Ther 26(1), 81-92 (2018)

Imaging Cancer Metabolism

Milica Momcilovic and David B. Shackelford*

Division of Pulmonary and Critical Care Medicine, David Geffen School of Medicine, Los Angeles, CA, 90095, USA

Abstract

It is widely accepted that altered metabolism contributes to cancer growth and has been described as a hallmark of cancer. Our view and understanding of cancer metabolism has expanded at a rapid pace, however, there remains a need to study metabolic dependencies of human cancer *in vivo*. Recent studies have sought to utilize multi-modality imaging (MMI) techniques in order to build a more detailed and comprehensive understanding of cancer metabolism. MMI combines several *in vivo* techniques that can provide complementary information related to cancer metabolism. We describe several non-invasive imaging techniques that provide both anatomical and functional information related to tumor metabolism. These imaging modalities include: positron emission tomography (PET), computed tomography (CT), magnetic resonance imaging (MRI), magnetic resonance spectroscopy (MRS) that uses hyperpolarized probes and optical imaging utilizing bioluminescence and quantification of light emitted. We describe how these imaging modalities can be combined with mass spectrometry and quantitative immunochemistry to obtain more complete picture of cancer metabolism. *In vivo* studies of tumor metabolism are emerging in the field and represent an important component to our understanding of how metabolism shapes and defines cancer initiation, progression and response to treatment. In this review we describe *in vivo* based studies of cancer metabolism that have taken advantage of MMI in both pre-clinical and clinical studies. MMI promises to advance our understanding of cancer metabolism in both basic research and clinical settings with the ultimate goal of improving detection, diagnosis and treatment of cancer patients.

Key Words: Tumor metabolism, Pet imaging, Mass spectrometry, Optical imaging

INTRODUCTION

Current view of cancer metabolism

The seminal work by Otto Warburg defined glycolysis under aerobic conditions as the basis of cancer metabolism (Warburg, 1956a). His primary basis for excess glucose metabolism was postulated to be a result of impaired mitochondria metabolism. While correct in the context of his working models, Warburg dismissed parallel studies from Sidney Weinhouse that accurately described oxidation of carbohydrates and fatty acids within tumors (Weinhouse *et al*., 1951). Weinhouse had discovered that tumors had active enzymes within the TCA cycle comparable to normal tissue (Wenner *et al*., 1952). These studies suggested that tumors in fact rely on metabolic pathways intrinsic to mitochondria. The two scientists – Warburg and Weinhouse disagreed on the basis of cancer metabolism and articulated these differences in a historic publication in Science in 1956 (Warburg, 1956b; Weinhouse, 1956). Their disagreement raised an important question – what metabolites do tumors use to sustain rapid anabolic growth? Today our understanding of cancer metabolism is that it is a heterogeneous process classically delineated by aerobic glycolysis but also equally dependent on mitochondrial metabolism for tumor growth (Desjardins *et al*., 1985; Morais *et al*., 1994; Cavalli *et al*., 1997; Weinberg *et al*., 2010).

Our view of tumor metabolism defined by Otto Warburg (Warburg *et al*., 1927) and coined by Efraim Racker in 1972 as the "Warburg Effect" (Racker, 1972) has been much refined, deepened and broaden enough that we may accept both Warburg and Weinhouse were correct, given the metabolic heterogeneity of their tumor models. For more reading on the life of Otto Warburg and the impact his research has had on the field of cancer metabolism please refer to an excellent review by Chi Dang and colleagues (Koppenol *et al*., 2011). The last two decades have marked a wave of studies dissecting the genetic, molecular and environmental basis of altered metabolism in cancer cells. Given that tumors show tremendous mutational heterogeneity, it is not surprising that they would likewise

Open Access **https://doi.org/10.4062/biomolther.2017.220**

Received Oct 24, 2017 **Revised** Nov 11, 2017 **Accepted** Nov 13, 2017
Published Online Dec 7, 2017

***Corresponding Author**
E-mail: DShackelford@mednet.ucla.edu
Tel: +310-267-2725, Fax: +310-206-8622

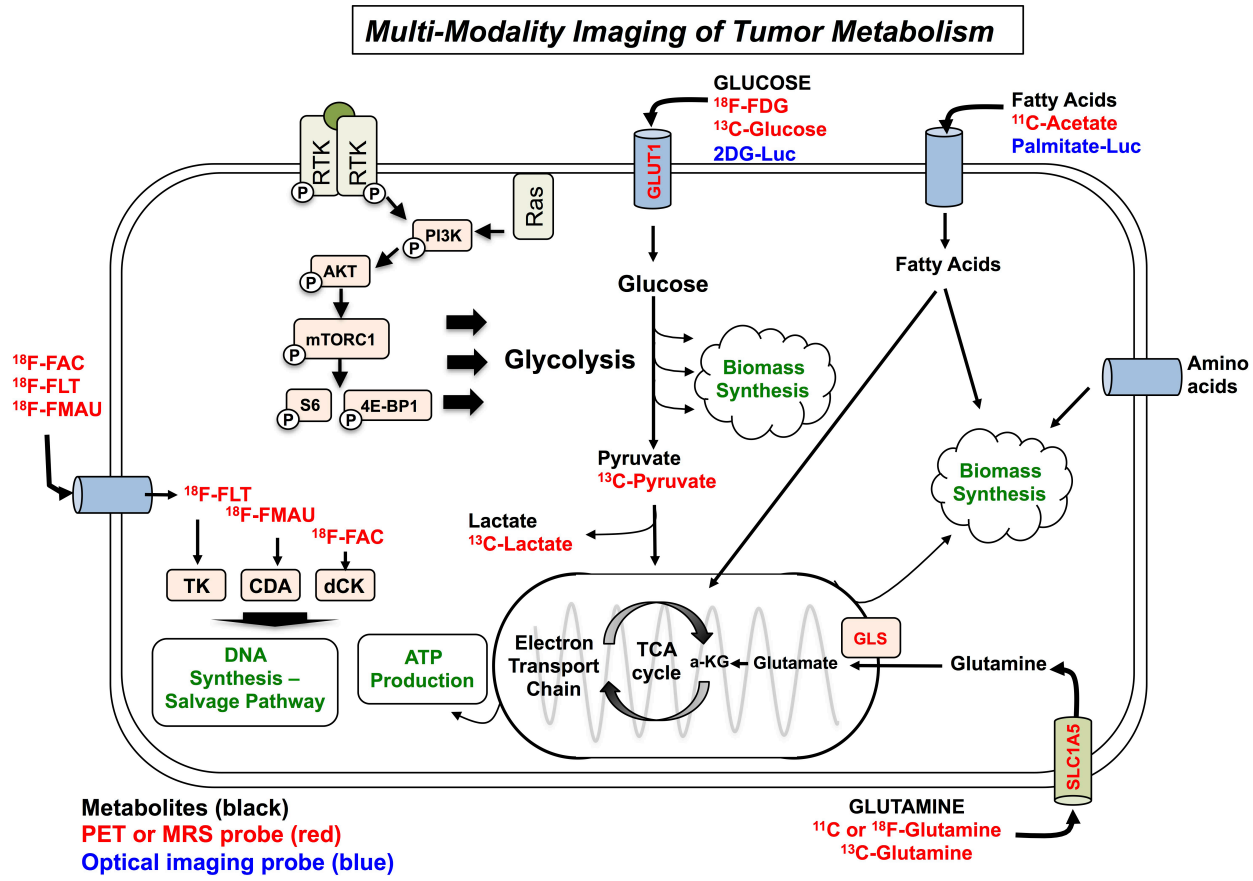

Fig. 1. Overview of major metabolic pathways that can be detected using different imaging modalities. Glucose uptake can be detected using PET with ^{18}F-FDG; using SIRM or MRS with ^{13}C-Glucose; using 2DG probes for optical imaging. Contribution of pyruvate and lactate to TCA cycle can be measured using SIRM or MRS with ^{13}C-Pyruvate and ^{13}C-Lactate. Glutamine uptake can be detected using PET with ^{18}F-Glutamine or ^{11}C-Glutamine; using SIRM with ^{13}C-Glutamine. Additional probes based on amino acids can be used to detect contribution of amino acids to cellular biomass synthesis. Fatty acid uptake by tumor cells can be evaluated using PET probe ^{11}C-Acetate or using optical imaging with luciferase-tagged free fatty acid. PET probes ^{18}F-FLT, ^{18}F-FAC, ^{18}F-FMAU can be used to determine reliance of tumors on thymidine kinase (TK) and/or deoxycitidine kinase (dCK) and/or cytidine deamidase (CDA). Combining imaging modalities with qIHC allows for quantification of total protein levels as well as phosphorylation.

show diverse metabolic heterogeneity. Tumors utilize a host of metabolites that include glucose, amino acids and fatty acids (Vander Heiden and DeBerardinis, 2017). However, the bulk of cancer metabolism studies have been confined to *in vitro* cell culture systems and require *in vivo* translation. Given our newly emerging vision of tumor metabolism as a multi-faceted and heterogeneous process how might we begin studying tumor metabolism through a different set of lenses? One answer lies in real time imaging of tumors.

In this review we will describe the use of multi-modality imaging (MMI) techniques that have been combinatorially used to quantitatively measure and assess tumor metabolism *in vivo* in both animal models of cancer and in cancer patients. We will describe noninvasive imaging modalities that include positron emission tomography (PET), magnetic resonance imaging (MRI) and magnetic resonance spectroscopy (MRS), computed tomography (CT) and optical imaging. We will also describe methods such as liquid chromatography and gas chromatography mass spectrometry (LC-MS and GC-MS) and quantitative immunohistochemistry (qIHC) that can be utilized to complement noninvasive imaging techniques.

OVERVIEW OF IMAGING MODALITIES TO STUDY CANCER METABOLISM

Positron emission tomography

Positron Emission Tomography (PET) imaging is a widely used imaging modality employed in both clinical and basic research settings. PET imaging works by detection of gamma rays from positron emitting radionuclides that have been injected into a patient or animal. The most commonly used radionuclide is ^{18}F but there is a wide range of radionuclides available – the more commonly used isotopes include ^{18}F, ^{11}C and ^{15}O. The high consumption of glucose by advanced tumors makes PET imaging with [^{18}F]fluro-2-deoxyglucose (^{18}F-FDG) an ideal probe to detect glycolytic tumors. ^{18}F-FDG works by entering the cell through glucose transporters (GLUTs) (Fig. 1) where it is rapidly phosphorylated by hexokinase into ^{18}F-FDG-6-phosphate where it can no longer be metabolized. Here the radiotracer remains trapped in the early stages of glycolysis allowing the detection of emitted gamma rays as the probe decays. Importantly, the 3 dimensional detection of

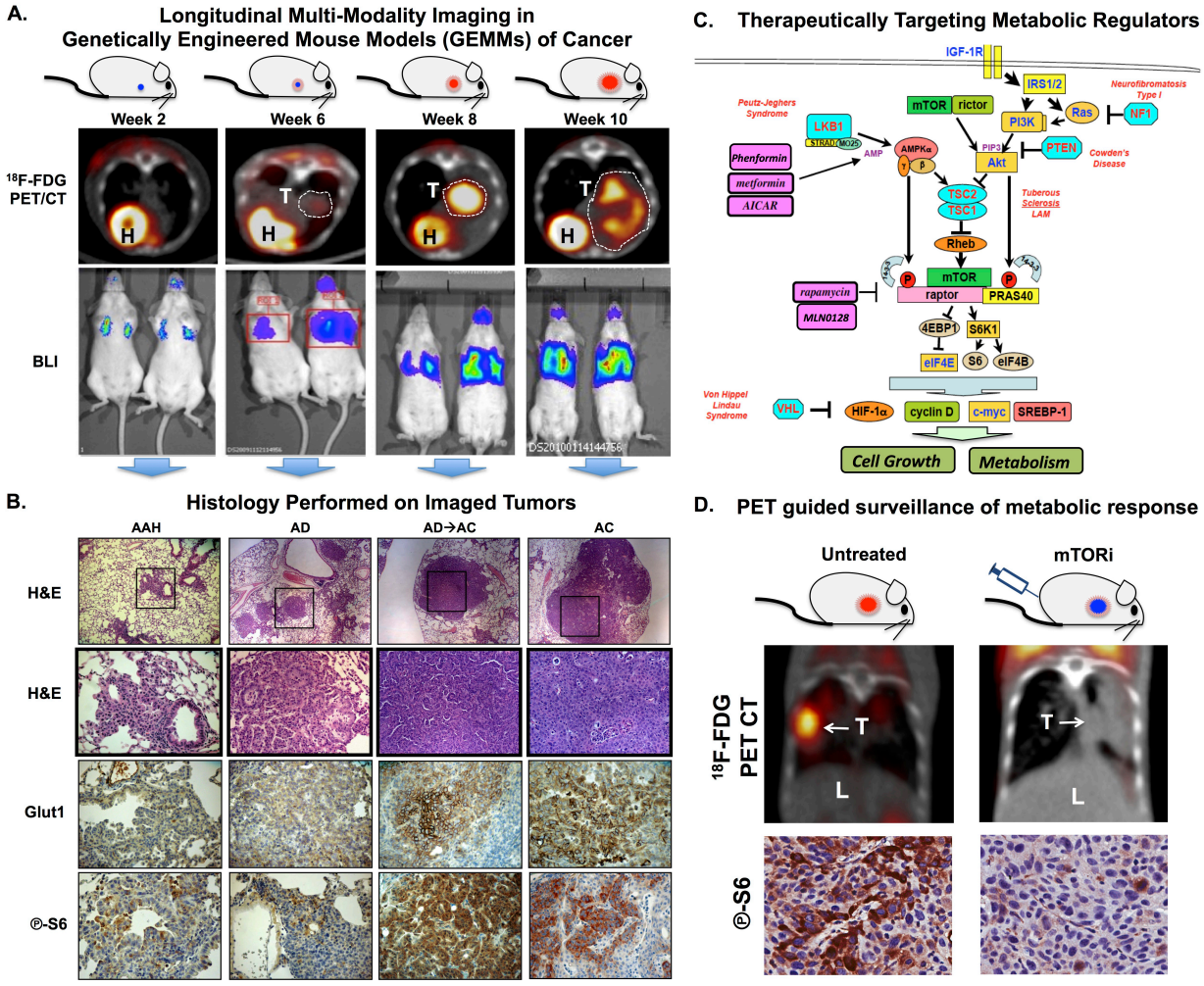

Fig. 2. Pre-clinical studies in mice using multi-modality imaging of tumor metabolism to guide targeted therapies (A) Overview of longitudinal ^{18}F-FDG PET/CT and BLI imaging of genetically engineered mouse model of lung cancer at 2, 6, 8 and 10 weeks post tumor induction. (B) Representative histology performed on mice imaged with PET/CT and BLI. Tumors were stained with H&E or Glut1 as a surrogate biomarker of glucose uptake or P-S6, a surrogate biomarker of mTORC1 signaling. (C) Representation of the PI3K/AKT/mTOR signaling pathway and its regulation of cellular growth and metabolism. In pink are metabolic based drugs and targeted therapies that target this pathway. (D) Representation of ^{18}F-FDG PET/CT guided studies in mice measuring metabolic response to the catalytic mTOR kinase inhibitor (mTORi). Top panel shows representative ^{18}F-FDG PET/CT images of mice untreated vs those treated with mTORi. Bottom panel shows representative immunohistochemical staining of lung tumors for the mTORC1 substrate.

gamma emission from a single source enables 3 dimensional reconstruction of the tumor. ^{18}F-FDG is used to successfully diagnose a broad range of tumors that include cancers of the lung, liver, bone and soft tissue (Minn *et al*., 1997; Oshida *et al*., 1998; Shiomi *et al*., 2001; Shi *et al*., 2015; Hwang *et al*., 2016).

^{18}F-FDG PET is particularly useful for metabolic studies because it measures glucose flux into the tumor and activity in early steps of glycolysis. While it also serves to detect a tumor mass, importantly it provides valuable functional information about the metabolic needs of the tumor. Moreover, when imaging cancer metabolism, it is critical to identify probes and modalities that provide, in addition to anatomical registration, functional information about the metabolic activity within the tumor(s). The noninvasive nature of PET imaging allows for repeat scans to be performed on patients during the course of treatment. The PET Response Criteria in Solid Tumors or PERCIST is a set of criteria that utilizes PET imaging with ^{18}F-FDG to determine therapeutic response in patients. The efficacy of PERCIST criteria was demonstrated in a clinical trial, which used ^{18}F-FDG uptake in tumors to evaluate breast tumor response to the PI3K inhibitor Buparlisib (Mayer *et al*., 2014). Likewise, longitudinal PET imaging of small animals is feasible and provides an accurate means to study tumor metabolism and measure therapeutic response over time. This is represented in Fig. 2A showing the longitudinal ^{18}F-FDG PET and CT imaging of Kras^{G12D} driven lung tumors in genetically engineered mouse models (GEMMs).

Tumors do not solely rely on glucose. Therefore radiolabeling of additional metabolites such as acetate, choline, methionine and glutamine with either ^{18}F or ^{11}C provide opportunities to perform broad profiling of cancer metabolism

with PET imaging. ^{11}C-acetate is converted to acetyl-CoA and used in mitochondria in TCA cycle or incorporated into cell membranes (Vavere *et al*., 2008; Yoshimoto *et al*., 2001) and along with ^{11}C- and ^{18}F-choline both are used in management of prostate cancer (Testa *et al*., 2016; Wibmer *et al*., 2016). ^{11}C-methionine is used as a marker of amino acid uptake and protein synthesis primarily in glioma where uptake of the radiotracer correlates with tumor grade (Pirotte *et al*., 2004; Kim *et al*., 2005; Van Laere *et al*., 2005). ^{11}C and ^{18}F-glutamine have been used in both clinical and basic research to evaluate reliance of tumor cells on glutamine uptake and glutaminolysis (Lieberman *et al*., 2011; Ploessl *et al*., 2012; Wu *et al*., 2014; Venneti *et al*., 2015; Hassanein *et al*., 2016; Momcilovic *et al*., 2017; Schulte *et al*., 2017; Zhou *et al*., 2017).

Computed tomography

Computed tomography (CT) imaging utilizes multi-positional X-ray imaging to generate a 3 dimensional view of the imaged area. Tomographic reconstruction of the X-ray images provides detailed anatomical information of the imaged patient or animal. CT imaging can be performed with contrast agents that register vasculature within the tumor and perfusion within the tumor(s). CT imaging with iodine based contrast agents such as iohexol, iodixanol and ioversol are advantageous because it renders a quantitative measure of blood vessels supplying the tumors (Kao *et al*., 2003; Mukundan *et al*., 2006; Karathanasis *et al*., 2009; de Vries *et al*., 2010).

Tumor vasculature directly impacts the nutrients accessible to the tumors and can be used to differentiate well-perfused regions from hypoxic regions. Recent study has evaluated contrast-enhanced CT with HX4-PET, PET probe specific for hypoxia. This study showed that in lung cancer patients both modalities were able to classify tumors as normoxic or hypoxic (Even *et al*., 2017). These imaging technologies are widely available for basic research and clinical use. However, since CT imaging exposes both patients and animals to ionizing radiation, the frequency of repetitive imaging must be taken into consideration for both clinical evaluation and studies in animal models (Brenner and Hall, 2007). Excessive exposure to radiation can be avoided by opting for low dose CT scans that provide accurate anatomical registration and patient benefit (National Lung Screening Trial Research Team *et al*., 2011, 2013; Rampinelli *et al*., 2013; Kubo *et al*., 2016).

Magnetic resonance imaging and spectroscopy

Magnetic Resonance Imaging (MRI) is based on the physical phenomenon called nuclear magnetic resonance (NMR). NMR is based on quantifying changes in nuclear spin, a property of atomic nuclei, in response to a strong external magnetic field. NMR signal is detected upon relaxation of nuclear spins. For imaging metabolism most useful nuclei are ^{1}H, ^{13}C and ^{31}P. Like CT imaging, MR imaging is most frequently used to determine anatomical registration of the tumor. In addition, MRI can be performed with contrast agents to determine perfusion within the tumor (Yankeelov and Gore, 2009).

Most commonly Magnetic Resonance Spectroscopy (MRS) has been used to evaluate endogenous ^{1}H signals from choline-containing molecules. Signal intensity of the ^{1}H MRS peak has correlated with proliferation in brain, prostate, breast, colon and cervical cancers (Nelson *et al*., 2002; Geraghty *et al*., 2008; Kurhanewicz and Vigneron, 2008; Haddadin *et al*., 2009; Mountford *et al*., 2009). One of the limitations of 1H MRS imaging is low sensitivity, with concentration of endogenous metabolites required to be in the high micromolar to millimolar range (Di Gialleonardo *et al*., 2016). In order to address the relatively low sensitivity of MRS imaging, a novel method for producing hyperpolarized probes has been developed (Ardenkjaer-Larsen *et al*., 2003; Golman *et al*., 2006). Hyperpolarization of ^{13}C nuclei has allowed for increase in the signal to noise ratio and detection sensitivity with up to 10,000-fold enhancement compared to conventional MRI (Ardenkjaer-Larsen *et al*., 2003; Keshari and Wilson, 2014).

Hyperpolarized [1-^{13}C]-pyruvate has been used to detect levels of lactate and alanine as well as total amount of hyperpolarized ^{13}C in preclinical models of prostate cancer (Albers *et al*., 2008). Furthermore, hyperpolarized ^{13}C-pyruvate was successfully applied to 31 patients with prostate cancer with excellent safety profile and spectral quality (Nelson *et al*., 2013). Data obtained from ^{13}C-pyruvate was able to accurately delineate the presence, location and size of cancer relative to surrounding non-cancer tissue. Moreover, MRS imaging is able to detect not only ^{13}C-pyruvate itself, but also metabolites downstream of pyruvate such as lactate and alanine. This greatly expands usefulness of the probe in measuring metabolism. In addition to detection and quantification of uptake of the initial probe, quantifying downstream metabolites allows for the estimation of enzyme activity and the estimation of activity of entire pathways in tumors (Gutte *et al*., 2015).

As with other modalities of non-invasive imaging, monitoring response to therapy is one of the most promising aspects of MRS imaging. In a pre-clinical model of lymphoma, ^{13}C-pyruvate was used to show that loss of flux from pyruvate to lactate correlated with response to chemotherapy (Day *et al*., 2007). Increased lactate signal was observed at sites of cancer recurrence in a MYC-driven murine breast cancer model (Shin *et al*., 2017). Additionally, ^{13}C-labeled acetate was used in pre-clinical models of glioblastomas and in brain tumor patients illustrating that tumors can oxidize acetate in addition to glucose (Mashimo *et al*., 2014). As with each imaging modality and technology, MRS imaging with hyperpolarized probes will benefit from further development of technology to improve generation and delivery of the probe to patients.

Optical imaging

Optical imaging is a widely used modality in basic research laboratories that measures and quantifies emission of visible light and wavelengths in near infrared spectrum. Optical imaging can be done in both fluorescent and bioluminescent models. Fluorescence imaging of dyes and proteins such as green fluorescent protein (GFP) has a low signal to noise ratio, due to the emission of light within the visible spectrum by cellular proteins and DNA. This has been improved upon with the development of fluorescent probes with emission in the near infrared spectrum (Zhang *et al*., 2012). The problem of signal to noise is absent in bioluminescent imaging (BLI) of cells and rodent models of disease since mammalian tissue does not spontaneously generate light.

Bioluminescence is a natural phenomenon observed across numerous species from bacteria, to worms to beetles to fireflies in which the luciferase enzyme catalyzes a reaction that releases photons of light. First taking advantage of the luciferase enzyme from fireflies, researchers were able to clone luciferase and introduce it as a reporter in cell lines and transgenic animals (Fan and Wood, 2007; Woolfenden *et*

al., 2009). BLI is highly sensitive and can detect fewer than 10 injected cells in a mouse using enhanced firefly luciferase (Rabinovich *et al*., 2008; Kim *et al*., 2010). BLI has most frequently been used as a noninvasive means to detect implanted tumors and to follow metastases in mouse xenografts. In addition, stable luciferase reporters have been introduced into genetically engineered mouse models (GEMMs) in which the luciferase gene is placed under a lox-stop-lox regulated endogenous promoter such as the Rosa26 locus (Safran *et al*., 2003). The lox-stop-lox regulated luciferase reporters are activated simultaneously with tumor induction and serve as an effective reporter of tumor growth, where the amount of light emission by BLI is proportional to the tumor burden (Fig. 2A).

The sensitivity of BLI enables small tumor lesions to be detected at early stages of tumorigenesis that fall below the level of detection for CT, MRI and PET imaging (Shackelford *et al*., 2013; Stollfuss *et al*., 2015). This is highlighted in Fig. 2A comparing ^{18}F-FDG PET and BLI of lung tumor lesions at 2-10 weeks post tumor induction. A limitation of BLI is the lack of 3 dimensional resolution. Therefore, the BLI can give a general estimate of tumor mass, but it cannot discern between single vs multiple tumor nodules. In contrast PET, CT and MR imaging provide an accurate 3 dimensional spatial mapping of the tumor and surrounding tissue but is limited in its ability to detect early stage small neoplasias. In a study comparing both ^{18}F-FDG PET and BLI in animal models of metastatic breast cancer the authors concluded that both imaging modalities were complementary (Kang *et al*., 2015).

Imaging with D-luciferin can detect the presence of tumors, but can BLI be used to study functional metabolism? BLI using luciferase can be used to measure ATP levels, allowing for the estimation of the energetic charge within the cell. This is based on the fact that reaction catalyzed by luciferase requires ATP, thus emitted light can be correlated to the amount of ATP available (Kimmich *et al*., 1975; Morciano *et al*., 2017). A limited number of bioluminescent and fluorescent probes have been developed to study metabolic pathways in cancer in more detail. Both glucose and free fatty acid analogs have been developed to study both glucose and fatty acid metabolism shown in Fig. 1 (Zhou *et al*., 2009; Henkin *et al*., 2012). Moreover, the use of bioorthogonal chemistry also known as 'click' chemistry enables the design of functional luciferin probes that can be activated by cellular metabolites and enzymes. Several recent studies utilized a luciferin probe conjugated to the free fatty acid palmitate to measure *in vivo* uptake and reduction in brown adipose tissue (Jang *et al*., 2016; Lynes *et al*., 2017). Here a cleavable disulfide bond links palmitate to luciferin. In the uncleaved form, palmitate acts as a cage to restrict luciferin from being catalyzed by the luciferase enzyme, which is expressed as a reporter gene. The caged luciferin is rendered inert until entry into the cell. Upon import of the probe into the cell, the disulfide bond is reduced and cleaved thus resulting in uncaging of the luciferin and subsequent catalysis by the luciferase reporter (Henkin *et al*., 2012). The amount of light detected following activation of the probe is proportional to the uptake of palmitate by the tissue being imaged. The development of caged luciferins that measure import of metabolites and enzyme activity represent a potential emerging technology that may integrated into *in vivo* studies of cancer metabolism.

COMPLEMENTARY METHODS TO NONINVASIVE IMAGING OF TUMOR METABOLISM

Mass spectrometry-based isotopomeric metabolic tracing

Metabolomics refers to the global study of metabolism and can be examined using multiple techniques. While technologies such as gene set enrichment analysis (GSEA) and protein expression can be used to profile the tumor's global metabolic profile (Nielsen, 2017), this review will focus on direct analysis of metabolites using Stable Isotope Resolved Metabolomics (SIRM). This technique utilizes liquid chromatography mass spectrometry (LC-MS) or gas chromatography mass spectrometry (GC-MS) as a direct means to measure the distribution of labeled metabolites. It takes advantage of low abundance in the cells and tissues of 13C and 15N isotopes compared to high abundance of natural isotopes 12C and 14N. This selectivity is coupled to extremely high sensitivity of detection of stable 13C and 15N isotopes offered by mass spectrometry. Employing SIRM allows tracing of the metabolic fate of the individual atoms from the labeled molecule. This means that as labeled molecule undergoes transformation in a metabolic pathway its contribution to each step of the pathway can be accurately quantified. A number of 13C- and 15N-labeled molecules are commercially available (for example ^{13}C-glucose, ^{13}C- and ^{15}N-glutamine, ^{13}C-palmitate) making it possible to study the fate of an individual metabolite as it is processed through multiple enzymatic steps in the cell.

The Fan laboratory has published a number of pioneering studies using SIRM technology in lung cancer cell lines (Fan *et al*., 2004, 2006) and more importantly on human lung cancer isolated from resected tumors (Fan *et al*., 2009). These studies demonstrated the translatability of the SIRM from basic research models into human patients. Several studies from the Vander Heiden lab have performed *in vivo* SIRM analysis using mouse models that identified distinct metabolic dependencies in Kras driven tumors (Davidson *et al*., 2016; Mayers *et al*., 2016). The DeBerardinis lab extended these findings by performing SIRM analysis on human non-small cell lung cancer. Quantification of glycolysis in tumors identified that metabolic heterogeneity within tumors can lead to different preference for carbon courses (Hensley *et al*., 2016). These findings bring forward an important question: do areas of the tumor that rely on the different carbon sources have different responses to standard therapy, whether it be chemotherapy, immunotherapy or targeted therapy?

Additional mass spectrometry based approaches have taken advantage of 'click' chemistry to design probes such as MitoClick that measure mitochondrial membrane potential (Logan *et al*., 2016). The mitochondrial membrane potential is maintained by the electron transport chain and serves to drive the generation of ATP by complex V. The MitoClick probe is voltage dependent and will accumulate in the inner mitochondrial membrane when a mitochondrial membrane potential is present. Quantification of MitoClick was performed using LC-MS of cardiac tissue in mice and although this probe cannot be analyzed by noninvasive methods, it does highlight a novel use of click chemistry and LC-MS to study mitochondrial bioenergetics *in vivo*.

Quantitative immunohistochemistry of signal transduction pathways

The use of bright field microscopy has been a staple of his-

tological analysis of tumor tissue for decades and is widely used by clinical pathology as well as basic research laboratories. Quantitative immunohistochemical (qIHC) staining of key signaling proteins and metabolic enzymes that regulate metabolism can readily be performed on formalin fixed paraffin embedded (FFPE) tumor sections in both human and mouse tumors. Fig. 1 represents signaling kinases within pathways such as the PI3K/AKT/mTOR signaling axis that function as critical regulators of glycolysis (Elstrom *et al*., 2004; Duvel *et al*., 2010; Hu *et al*., 2016). The bulk of these kinases are activated through phosphorylation of serine, threonine and tyrosine residues making them amenable to detection using phospho-specific antibodies. This allows for on-off rates of these enzymes to be measured in primary, FFPE tumor tissue.

To quantify IHC staining, slides are digitally scanned and staining intensity can be quantified using morphometric software. Next, druggable targets can be identified and treated with targeted therapies. Fig. 2B shows IHC staining of the mTORC1 substrate phospho-S6 (P-S6) is elevated in lung tumors isolated from Kras/Lkb1 mutant GEMMs. The signaling pathway and several druggable targets are summarized in Fig. 2C. Our laboratory has performed pre-clinical *in vivo* studies in GEMMs targeting lung tumors that have hyper-active mTORC1 signaling with the mTOR inhibitor MLN128 (Momcilovic *et al*., 2015). This study was conducted using a combined analysis of ^{18}F-FDG PET to measure glucose metabolism and IHC staining of mTOR substrates P-S6 and P-4EBP1 to measure inhibition of mTOR signaling. We detected lower ^{18}F-FDG signal in tumors that received MLN128 and this correlated with lower P-S6 staining in the same tumors compared to untreated tumors (Fig. 2D). Further validating this approach, ^{18}F-FDG PET was successfully used to guide a study targeting NF1 mutant tumors. Here the authors mapped both the mTOR and MAPK signaling pathways as critical regulators of tumor metabolism and survival (Malone *et al*., 2014). NF1 mutant tumors were highly responsive to combined inhibition of both these signaling nodes resulting in reduced tumor growth and glucose uptake in tumors as measured by ^{18}F-FDG PET.

INTEGRATING MULTIPLE IMAGING MODALITIES TO PROFILE TUMOR METABOLISM *IN VIVO*

Coupling PET and CT imaging to mass spectrometry

While noninvasive ^{18}F-FDG PET imaging provides both spatial and temporal assessment of glycolysis at different stages of tumorigenesis, this modality does not inform us of the fate of glucose beyond early steps of glycolysis. Therefore, by coupling ^{18}F-FDG PET imaging to SIRM analysis using LC-MS of ^{13}C-glucose one can attain a comprehensive picture of glucose uptake and glucose utilization within the cell. Examples of this type of approach are highlighted in a study examining the role of Kras dependent metabolism in pancreatic ductal adenocarcinoma (PDAC) (Ying *et al*., 2012). Here the authors performed ^{18}F-FDG PET on pancreatic tumors in a Kras^{G12D} driven PDAC mouse model followed by LC-MS analysis of ^{13}C-glucose on mouse derived PDAC cell lines. Additional analysis using qIHC identified the MAPK signaling pathway as a critical driver of glycolysis in PDAC. Subsequent studies have shown the feasibility of *in vivo* metabolite analysis by infusing either mice or patients with ^{13}C-glucose and isolating tumors for *ex vivo* LC-MS analysis (Davidson *et al*., 2016; Hensley *et al*., 2016).

Imaging mice with two different PET probes on consecutive days was performed using ^{18}F-FDG and ^{18}F-Glutamine in order to evaluate glucose and glutamine uptake in tumors. Venetti *et al*., demonstrated usefulness of ^{18}F-Glutamine over ^{18}F-Glucose in imaging gliomas in both mouse models and in human patients (Venneti *et al*., 2015). ^{18}F-Glutamine had superior tumor-to-background ratio compared to ^{18}F-FDG, allowing clear tumor delineation. Recent reports showed that both ^{18}F-FDG and ^{18}F-Glutamine or ^{11}C-Glutamine are consumed by EGFR mutant lung adenocarcinomas suggesting metabolic dependency on both glucose and glutamine in this subset of lung cancer (Hassanein *et al*., 2016; Momcilovic *et al*., 2017). Moreover, ^{18}F-Glutamine and ^{11}C-Glutamine uptake correlated with levels of the glutamine transporter ASCT2 (also known as SLC1A5), which was detected by IHC.

Imaging tumor metabolism with hyperpolarized MRS

Hyperpolarized ^{13}C-Pyruvate has been used in multiple preclinical studies of lymphoma (Day *et al*., 2007; Dutta *et al*., 2013), prostate cancer (Keshari *et al*., 2013), glioblastoma (I. Park *et al*., 2011; Chaumeil *et al*., 2012), pancreatic cancer (Rajeshkumar *et al*., 2015; Serrao *et al*., 2016) and breast cancer (Shin *et al*., 2017). Hyperpolarized ^{13}C-Glutamine has also been used in pre-clinical models of prostate cancer (Canape *et al*., 2015), liver cancer (Cabella *et al*., 2013; Gallagher *et al*., 2008), glioma (Qu *et al*., 2011) and IDH1/2 mutant chondrosarcoma (Salamanca-Cardona *et al*., 2017). Similarly, use of hyperpolarized ^{13}C-Glucose has been reported in mouse lymphoma cell line (Timm *et al*., 2015), mouse lymphoma and lung tumors (Rodrigues *et al*., 2014). While still early in development, MRS is a new technique that has great potential in clinical application. This was demonstrated by successful application in patients with prostate cancer in which ^{13}C-pyruvate and its metabolic products lactate, alanine and bicarbonate were measured in tumors using MRS imaging (Nelson *et al*., 2013). Please refer to an excellent review by Salmanca-Cardona and Keshari (2015) for an in depth summary of nuclear polarization-enhanced MR imaging.

Profiling metabolic phenotypes in tumors with PET and optical imaging

Multi-modality imaging in preclinical mouse studies has routinely combined PET/CT with BLI bringing together sensitivity of PET to detect metabolic activity within tumors with sensitivity of BLI for detection of small number of cells. Pioneering studies by the Gambhir lab, demonstrated that combining ^{18}F-FDG/CT imaging with BLI was an effective and sensitive method to study tumor metabolism (Deroose *et al*., 2007). Their laboratory has recently extended the application of PET and BLI multi-modality imaging in an orthotopic mouse model of human glioma to investigate a novel radiotracer, ^{11}C-DASA-23 that directly measures activity of pyruvate kinase M2 isoform (PKM2) *in vivo* (Witney *et al*., 2015). Our lab has successfully utilized ^{18}F-FDG/CT and BLI imaging to identify early stage tumors in GEMMs and to monitor therapeutic response (Shackelford *et al*., 2013; Momcilovic *et al*., 2015). The addition of bioluminescence or fluorescence imaging probes to PET imaging can help delineate changes in tumor metabolism in response to therapy before any changes in tumor volume become apparent (Tseng *et al*., 2017).

Optical imaging represents a cost effective alternative

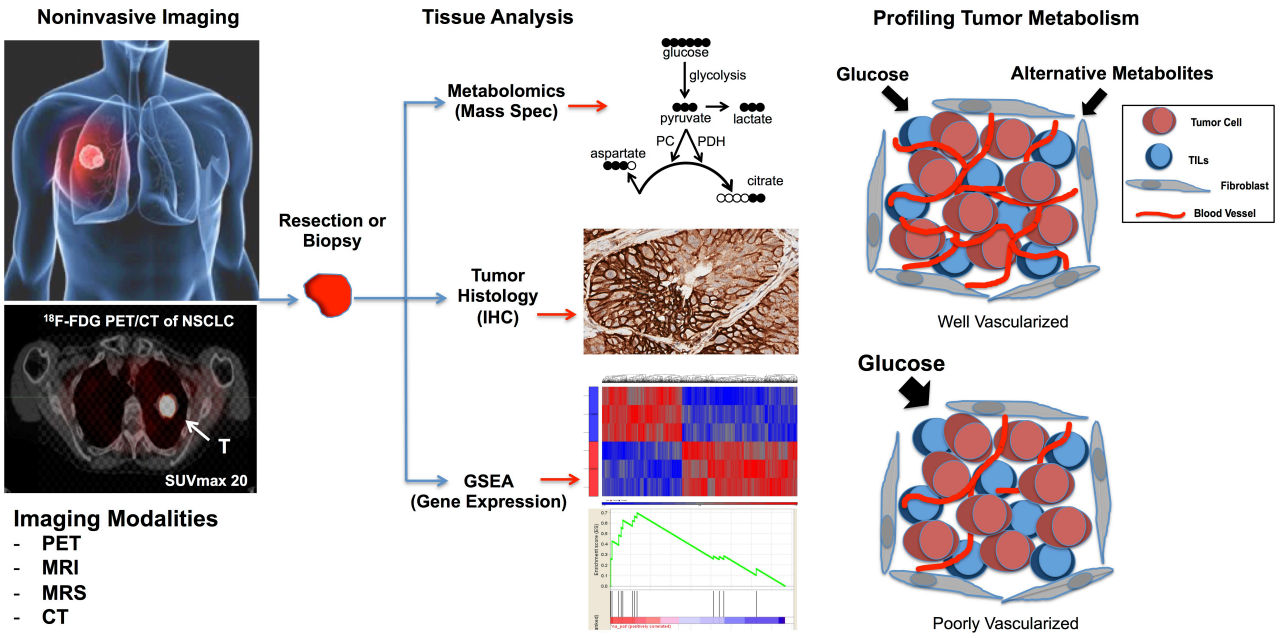

Fig. 3. Comprehensive profiling of tumor metabolism. Following non-invasive imaging with PET, MRI, MRS, CT patients undergo resection or biopsy of the tumor. Tissue analysis of the resected or biopsied tumor includes metabolomics, qIHC and gene expression analysis. Comprehensive tumor profiling identified preference for glucose in poorly vascularized areas of the tumor, compared to well vascularized tumors that used both glucose and alternative metabolites to fuel their growth.

to more costly approaches such as PET and MRS imaging. Moreover, recent studies have demonstrated that caged luciferin probes can be designed to detect metabolite or enzyme activity (Wehrman *et al*., 2006; Yao *et al*., 2007; Dragulescu-Andrasi *et al*., 2009; Hickson *et al*., 2010; Van de Bittner *et al*., 2010; Scabini *et al*., 2011; Jang *et al*., 2016; Lynes *et al*., 2017; Park *et al*., 2017). Optical imaging with bioluminescence requires the presence of reporters in cell lines and mouse models of cancer and at first glance appears not directly translatable into clinical applications. However, intraoperative fluorescent imaging is used in surgical oncology to aid in visualization of tumors and complete resection of the tumors and may have applications in cancer metabolism in the future (Vahrmeijer *et al*., 2013; van Oosten *et al*., 2013; Mondal *et al*., 2014; Landau, Gould, & Patel, 2016; Dworsky *et al*., 2017).

Multi-modality imaging of tumor metabolism in cancer patients

Is it possible to translate MMI imaging from pre-clinical studies in mice to cancer patients? Yes. This was recently demonstrated in a seminal study by the DeBerardinis laboratory in which they profiled glucose metabolism in human lung cancer patients using MMI coupled to detailed metabolic and molecular analysis (Hensley *et al*., 2016). Here the authors coupled ^{18}F-FDG PET and MRI with LC-MS and IHC to comprehensively profile tumor metabolism in patients undergoing surgical resection of tumors. The work-flow of this MMI analysis is represented in Fig. 3. The authors utilized ^{18}F-FDG PET to inform them of the tumor's glucose uptake and MRI with contrast to differentiate well-perfused regions from avascular hypoxic regions. The patients were infused with ^{13}C labeled glucose followed by LC-MS metabolomic analysis of resected tumor. In addition, IHC staining and gene expression analysis were performed on the tumor to score parameters such as expression of metabolic enzymes, tumor histology, tumor grade and tumor proliferation index. What the authors discovered was that tumor metabolism is heterogeneous within a single tumor and across individual tumors. They found that well perfused lung tumors utilized glucose and alternative nutrients while tumors with low perfusion relied primarily on glucose (Fig. 3).

Multi-modality imaging to guide therapy

Can profiling tumor metabolism improve cancer treatment? Tumor metabolism is recognized as a hallmark of cancer therefore characterizing the metabolic phenotype of the tumor is an important first step in diagnosis and treatment. Tumor metabolism informs us of the anabolic growth rate of the tumor and its capacity for continued growth. Importantly, metabolic profiling provides functional analysis of the tumor. Furthermore, coordinating PET with LC-MS and qIHC will serve to identify metabolic dependencies and druggable proteins within tumors that can be inhibited with targeted therapies or even combined with immune based therapies. Metabolic profiling performed on human NSCLC revealed tumor metabolism is heterogeneous, suggesting that combination treatments will be required. However, in order for metabolic therapies to successful target a tumor, first the metabolic dependencies must be identified. If a tumor uses a multitude of metabolites as its fuel source then a treatment strategy that inhibits only one metabolite such as glucose is predicted to fail. By profiling tumors noninvasively with MMI and validating with metabolomics, researchers and clinicians will be able to take a snap shot of the tumor's metabolic dependencies. This will allow for design of precise therapies that inhibit key metabolic nodes. The non-invasive nature of PET and MRS imaging means that repeat

imaging will be possible with the goal of this imaging informing oncologists and radiologists of treatment efficacy and course of action.

This was demonstrated recently in $Kras^{G12D}$ driven GEMMs of lung cancer treated with the glutaminase (GLS) inhibitor CB-839. As a single therapy, CB-839 failed to have any impact on tumor growth because these tumors are not dependent upon glutamine metabolism (Davidson *et al*., 2016). $Kras^{G12D}$ driven tumors readily adapt their metabolism to treatment and oncogenic stress as shown in a study examining metabolic response to $Kras^{G12D}$ ablation in a PDAC mouse model. Here the authors demonstrated that tumors adapt to inhibition of glucose metabolism by upregulation of oxidative mitochondrial metabolism following suppression of oncogenic $Kras^{G12D}$ (Viale *et al*., 2014). Conversely, $Kras^{G12D}$ driven tumors treated with biguanides, which are mitochondria complex I inhibitors that suppress oxidative phosphorylation (OXPHOS), induced up regulation of glycolysis as a compensatory mechanism that is readily detected by ^{18}F-FDG PET imaging (Dykens *et al*., 2008; Shackelford *et al*., 2013). Combined inhibition of both glycolysis and oxidative phosphorylation potently suppressed $Kras^{G12D}$ driven lung and pancreatic tumors (Momcilovic *et al*., 2015; Viale *et al*., 2014).

Distinct populations of tumors such as lung adenocarcinomas driven by EGFR mutations or triple negative breast cancer have shown dependency on glutamine metabolism *in vivo* and responsiveness to CB-839 treatment (Gross *et al*., 2014). PET imaging based profiling of EGFR mutant lung tumors with ^{18}F-FDG and ^{18}F-Glutamine or ^{11}C-Glutamine radiotracers suggested a dual dependency on both glucose and glutamine *in vivo* and predicted sensitivity to combined inhibition of glucose and glutamine metabolism (Qu *et al*., 2012; Hassanein *et al*., 2016; Momcilovic *et al*., 2017). Treatment of EGFR mutant lung tumors with the EGFR inhibitor erlotinib in combination with the GLS inhibitor CB-839 induced a potent anti-tumor response and tumor regression in mouse xenografts (Momcilovic *et al*., 2017). Additionally, a recent study showed that ^{18}F-glutamine was a predictive therapeutic biomarker of response in mouse models of BRAF mutant colorectal cancer (CRC) to single or combination inhibitors against the BRAF and PI3K signaling pathways (Schulte *et al*., 2017).

The importance of PET imaging in determining response to therapy was elegantly demonstrated using ^{18}F-FAC, a deoxycytidine kinase analog that is phosphorylated by deoxycytidine kinase (dCK) and incorporated in DNA synthesis pathway (Radu *et al*., 2008; Laing *et al*., 2009). ^{18}F-FAC had a better selectivity for lymphoid organs compared to ^{18}F-FDG and allowed for stratification and precise targeting of acute lymphoblastic leukemia (ALL) using targeted therapies against the ataxia telangiectasia and Rad3-related (ATR) protein and the dCK enzyme (Le *et al*., 2017). Two additional probes can be used to determine activity of enzymes involved in DNA salvage pathway. Tumor uptake of ^{18}F-FMAC relies on activity of cytidine deaminase (CDA) and uptake of ^{18}F-FLT is dependent on activity of thymidine kinase (TK) (Grierson and Shields, 2000; Lee *et al*., 2012). The importance of ^{18}F-FAC probe was further demonstrated in metabolomics based study in which LC-MS and ^{18}F-FAC uptake in liposarcomas identified dependency on nucleoside metabolism and successfully predicted sensitivity to gemcitabine treatment (Braas *et al*., 2012).

Open questions, challenges and future directions

Both PET and MRS imaging are costly ventures and often are not feasible on an academic budget. Can we identify and develop cost effective strategies to expand imaging in cancer metabolism in both pre-clinical and clinical studies? Development of optical imaging probes may provide a cost effective alternative to measure metabolism in tumors. However, development and careful validation of these probes will be required. Since caged luciferin probes rely on reporter-based systems their applications are restricted to pre-clinical studies. Combining multiple imaging platforms such as PET and MRI into single imaging units will likely increase the demand and throughput for pre-clinical imaging. Lastly, the availability of affordable radiotracers and hyperpolarized probes as well as micro-PET and MRS scanners hold promise to expand probe development and usage of MMI in the field of cancer metabolism. Miniaturized radiotracer development platforms such as ELIXYS may provide critical first steps towards wider availability of probes for basic and clinical research (Lazari *et al*., 2013).

Regardless of the imaging modality used, imaging of bulk tumors reflects a total sum from all cells in the tumor. Quantitative analysis within a heterogeneous tumor microenviroment presents a cadre of challenges. For example, what are the contributions of probe uptake for tumor supportive cells, such as stroma and tumor infiltrating leukocytes (TILs)? The recent success of immune based therapies in cancer have ushered in a wave of studies that have begun exploring the intersection of metabolism between the tumor and its microenvironment. It will be important to consider what proportion of the imaging signal is contributed by the tumor microenvironment contribute when imaging tumors with PET or MRS and validating with SIRM. Comparing the signal from bulk tumor to that of isolated tumor and immune cells may provide answers to these important questions.

SUMMARY AND CONCLUDING REMARKS

Metabolism is a fundamental cornerstone of PET and MRS imaging and represents a powerful tool to study tumor metabolism in basic research and clinical settings. Tumors are heterogeneous by nature and their metabolism reflects this. Since tumors utilize a host of metabolites beyond glucose it is conceivable that the future of PET and MRS imaging in patients will utilize a multitude of radiotracers and ^{13}C labeled metabolites to provide a detailed and real time signature of the tumor's metabolic profile. This signature promises to provide valuable information to guide precise and personalized treatments. The likely future of cancer treatment is to manage the disease chronically with cocktail therapies similar to what has been done for HIV patients. Here, MMI guided metabolic profiling would provide oncologists, radiologists and pathologists with a roadmap to how tumors adapt and how we can stay one step ahead with effective therapies.

REFERENCES

Albers, M. J., Bok, R., Chen, A. P., Cunningham, C. H., Zierhut, M. L., Zhang, V. Y., Kohler, S. J., Tropp, J., Hurd, R. E., Yen, Y. F., Nelson, S. J., Vigneron, D. B. and Kurhanewicz, J. (2008) Hyperpolar-

ized 13C lactate, pyruvate, and alanine: noninvasive biomarkers for prostate cancer detection and grading. *Cancer Res.* **68**, 8607-8615.

Ardenkjaer-Larsen, J. H., Fridlund, B., Gram, A., Hansson, G., Hansson, L., Lerche, M. H., Servin, R., Thaning, M. and Golman, K. (2003) Increase in signal-to-noise ratio of > 10,000 times in liquid-state NMR. *Proc. Natl. Acad. Sci. U.S.A.* **100**, 10158-10163.

Braas, D., Ahler, E., Tam, B., Nathanson, D., Riedinger, M., Benz, M. R., Smith, K. B., Eilber, F. C., Witte, O. N., Tap, W. D., Wu, H. and Christofk, H. R. (2012) Metabolomics strategy reveals subpopulation of liposarcomas sensitive to gemcitabine treatment. *Cancer Discov.* **2**, 1109-1117.

Brenner, D. J. and Hall, E. J. (2007) Computed tomography--an increasing source of radiation exposure. *N. Engl. J. Med.* **357**, 2277-2284.

Cabella, C., Karlsson, M., Canape, C., Catanzaro, G., Colombo Serra, S., Miragoli, L., Poggi, L., Uggeri, F., Venturi, L., Jensen, P. R., Lerche, M. H. and Tedoldi, F. (2013) *In vivo* and *in vitro* liver cancer metabolism observed with hyperpolarized [5-(13)C]glutamine. *J. Magn. Reson.* **232**, 45-52.

Canape, C., Catanzaro, G., Terreno, E., Karlsson, M., Lerche, M. H. and Jensen, P. R. (2015) Probing treatment response of glutaminolytic prostate cancer cells to natural drugs with hyperpolarized [5-(13) C]glutamine. *Magn. Reson. Med.* **73**, 2296-2305.

Cavalli, L. R., Varella-Garcia, M. and Liang, B. C. (1997) Diminished tumorigenic phenotype after depletion of mitochondrial DNA. *Cell Growth Differ.* **8**, 1189-1198.

Chaumeil, M. M., Ozawa, T., Park, I., Scott, K., James, C. D., Nelson, S. J. and Ronen, S. M. (2012) Hyperpolarized 13C MR spectroscopic imaging can be used to monitor Everolimus treatment *in vivo* in an orthotopic rodent model of glioblastoma. *Neuroimage* ***59***, 193-201.

Davidson, S. M., Papagiannakopoulos, T., Olenchock, B. A., Heyman, J. E., Keibler, M. A., Luengo, A., Bauer, M. R., Jha, A. K., O'Brien, J. P., Pierce, K. A., Gui, D. Y., Sullivan, L. B., Wasylenko, T. M., Subbaraj, L., Chin, C. R., Stephanopolous, G., Mott, B. T., Jacks, T., Clish, C. B. and Vander Heiden, M. G. (2016) Environment impacts the metabolic dependencies of ras-driven non-small cell lung cancer. *Cell Metab.* **23**, 517-528.

Day, S. E., Kettunen, M. I., Gallagher, F. A., Hu, D. E., Lerche, M., Wolber, J., Golman, K., Ardenkjaer-Larsen, J. H. and Brindle, K. M. (2007) Detecting tumor response to treatment using hyperpolarized 13C magnetic resonance imaging and spectroscopy. *Nat. Med.* **13**, 1382-1387.

de Vries, A., Custers, E., Lub, J., van den Bosch, S., Nicolay, K. and Grull, H. (2010) Block-copolymer-stabilized iodinated emulsions for use as CT contrast agents. *Biomaterials* **31**, 6537-6544.

Deroose, C. M., De, A., Loening, A. M., Chow, P. L., Ray, P., Chatziioannou, A. F. and Gambhir, S. S. (2007) Multimodality imaging of tumor xenografts and metastases in mice with combined small-animal PET, small-animal CT, and bioluminescence imaging. *J. Nucl. Med.* **48**, 295-303.

Desjardins, P., Frost, E. and Morais, R. (1985) Ethidium bromide-induced loss of mitochondrial DNA from primary chicken embryo fibroblasts. *Mol. Cell. Biol.* **5**, 1163-1169.

Di Gialleonardo, V., Wilson, D. M. and Keshari, K. R. (2016) The potential of metabolic imaging. *Semin. Nucl. Med.* **46**, 28-39.

Dragulescu-Andrasi, A., Liang, G. and Rao, J. (2009) *In vivo* bioluminescence imaging of furin activity in breast cancer cells using bioluminogenic substrates. *Bioconjug. Chem.* **20**, 1660-1666.

Dutta, P., Le, A., Vander Jagt, D. L., Tsukamoto, T., Martinez, G. V., Dang, C. V. and Gillies, R. J. (2013) Evaluation of LDH-A and glutaminase inhibition *in vivo* by hyperpolarized 13C-pyruvate magnetic resonance spectroscopy of tumors. *Cancer Res.* **73**, 4190-4195.

Duvel, K., Yecies, J. L., Menon, S., Raman, P., Lipovsky, A. I., Souza, A. L., Triantafellow, E., Ma, Q., Gorski, R., Cleaver, S., Vander Heiden, M. G., MacKeigan, J. P., Finan, P. M., Clish, C. B., Murphy, L. O. and Manning, B. D. (2010) Activation of a metabolic gene regulatory network downstream of mTOR complex 1. *Mol. Cell* **39**, 171-183.

Dworsky, E. M., Hegde, V., Loftin, A. H., Richman, S., Hu, Y., Lord, E., Francis, K. P., Miller, L. S., Wang, J. C., Scaduto, A. and Bernthal, N. M. (2017) Novel *in vivo* mouse model of implant related spine infection. *J. Orthop. Res.* **35**, 193-199.

Dykens, J. A., Jamieson, J., Marroquin, L., Nadanaciva, S., Billis, P. A. and Will, Y. (2008) Biguanide-induced mitochondrial dysfunction yields increased lactate production and cytotoxicity of aerobically-poised HepG2 cells and human hepatocytes *in vitro*. *Toxicol. Appl. Pharmacol.* **233**, 203-210.

Elstrom, R. L., Bauer, D. E., Buzzai, M., Karnauskas, R., Harris, M. H., Plas, D. R., Zhuang, H., Cinalli, R. M., Alavi, A., Rudin, C. M. and Thompson, C. B. (2004) Akt stimulates aerobic glycolysis in cancer cells. *Cancer Res.* **64**, 3892-3899.

Even, A. J. G., Reymen, B., La Fontaine, M. D., Das, M., Jochems, A., Mottaghy, F. M., Belderbos, J. S. A., De Ruysscher, D., Lambin, P. and van Elmpt, W. (2017) Predicting tumor hypoxia in non-small cell lung cancer by combining CT, FDG PET and dynamic contrast-enhanced CT. *Acta Oncol.* 1-6.

Fan, F. and Wood, K. V. (2007) Bioluminescent assays for high-throughput screening. *Assay Drug Dev. Technol.* **5**, 127-136.

Fan, T. W., Higashi, R. M. and Lane, A. N. (2006) Integrating metabolomics and transcriptomics for probing SE anticancer mechanisms. *Drug Metab. Rev.* **38**, 707-732.

Fan, T. W., Lane, A. N. and Higashi, R. M. (2004) The promise of metabolomics in cancer molecular therapeutics. *Curr. Opin. Mol. Ther.* **6**, 584-592.

Fan, T. W., Lane, A. N., Higashi, R. M., Farag, M. A., Gao, H., Bousamra, M. and Miller, D. M. (2009) Altered regulation of metabolic pathways in human lung cancer discerned by (13)C stable isotope-resolved metabolomics (SIRM) *Mol. Cancer* **8**, 41.

Gallagher, F. A., Kettunen, M. I., Day, S. E., Lerche, M. and Brindle, K. M. (2008) 13C MR spectroscopy measurements of glutaminase activity in human hepatocellular carcinoma cells using hyperpolarized 13C-labeled glutamine. *Magn. Reson. Med.* **60**, 253-257.

Geraghty, P. R., van den Bosch, M. A., Spielman, D. M., Hunjan, S., Birdwell, R. L., Fong, K. J., Stables, L. A., Zakhour, M., Herfkens, R. J. and Ikeda, D. M. (2008) MRI and (1)H MRS of the breast: presence of a choline peak as malignancy marker is related to K21 value of the tumor in patients with invasive ductal carcinoma. *Breast J.* **14**, 574-580.

Golman, K., Zandt, R. I., Lerche, M., Pehrson, R. and Ardenkjaer-Larsen, J. H. (2006) Metabolic imaging by hyperpolarized 13C magnetic resonance imaging for *in vivo* tumor diagnosis. *Cancer Res.* **66**, 10855-10860.

Grierson, J. R. and Shields, A. F. (2000) Radiosynthesis of 3'-deoxy-3'-[(18)F]fluorothymidine: [(18)F]FLT for imaging of cellular proliferation *in vivo*. *Nucl. Med. Biol.* **27**, 143-156.

Gross, M. I., Demo, S. D., Dennison, J. B., Chen, L., Chernov-Rogan, T., Goyal, B., Janes, J. R., Laidig, G. J., Lewis, E. R., Li, J., Mackinnon, A. L., Parlati, F., Rodriguez, M. L., Shwonek, P. J., Sjogren, E. B., Stanton, T. F., Wang, T., Yang, J., Zhao, F. and Bennett, M. K. (2014) Antitumor activity of the glutaminase inhibitor CB-839 in triple-negative breast cancer. *Mol. Cancer Ther.* **13**, 890-901.

Gutte, H., Hansen, A. E., Johannesen, H. H., Clemmensen, A. E., Ardenkjaer-Larsen, J. H., Nielsen, C. H. and Kjaer, A. (2015) The use of dynamic nuclear polarization (13)C-pyruvate MRS in cancer. *Am. J. Nucl. Med. Mol. Imaging* **5**, 548-560.

Haddadin, I. S., McIntosh, A., Meisamy, S., Corum, C., Styczynski Snyder, A. L., Powell, N. J., Nelson, M. T., Yee, D., Garwood, M. and Bolan, P. J. (2009) Metabolite quantification and high-field MRS in breast cancer. *NMR Biomed.* **22**, 65-76.

Hassanein, M., Hight, M. R., Buck, J. R., Tantawy, M. N., Nickels, M. L., Hoeksema, M. D., Harris, B. K., Boyd, K., Massion, P. P. and Manning, H. C. (2016) Preclinical evaluation of 4-[18F]Fluoroglutamine PET to assess ASCT2 expression in lung cancer. *Mol. Imaging Biol.* **18**, 18-23.

Henkin, A. H., Cohen, A. S., Dubikovskaya, E. A., Park, H. M., Nikitin, G. F., Auzias, M. G., Kazantzis, M., Bertozzi, C. R. and Stahl, A. (2012) Real-time noninvasive imaging of fatty acid uptake *in vivo*. *ACS Chem. Biol.* **7**, 1884-1891.

Hensley, C. T., Faubert, B., Yuan, Q., Lev-Cohain, N., Jin, E., Kim, J., Jiang, L., Ko, B., Skelton, R., Loudat, L., Wodzak, M., Klimko, C., McMillan, E., Butt, Y., Ni, M., Oliver, D., Torrealba, J., Malloy, C. R., Kernstine, K., Lenkinski, R. E. and DeBerardinis, R. J. (2016)

Metabolic heterogeneity in human lung tumors. *Cell* **164**, 681-694.
Hickson, J., Ackler, S., Klaubert, D., Bouska, J., Ellis, P., Foster, K., Oleksijew, A., Rodriguez, L., Schlessinger, S., Wang, B. and Frost, D. (2010) Noninvasive molecular imaging of apoptosis *in vivo* using a modified firefly luciferase substrate, Z-DEVD-aminoluciferin. *Cell Death Differ.* **17**, 1003-1010.
Hu, H., Juvekar, A., Lyssiotis, C. A., Lien, E. C., Albeck, J. G., Oh, D., Varma, G., Hung, Y. P., Ullas, S., Lauring, J., Seth, P., Lundquist, M. R., Tolan, D. R., Grant, A. K., Needleman, D. J., Asara, J. M., Cantley, L. C. and Wulf, G. M. (2016) Phosphoinositide 3-kinase regulates glycolysis through mobilization of aldolase from the actin cytoskeleton. *Cell* **164**, 433-446.
Hwang, J. P., Lim, I., Kong, C. B., Jeon, D. G., Byun, B. H., Kim, B. I., Choi, C. W. and Lim, S. M. (2016) Prognostic value of SUVmax measured by pretreatment Fluorine-18 fluorodeoxyglucose positron emission tomography/computed tomography in patients with ewing sarcoma. *PLoS ONE* **11**, e0153281.
Jang, C., Oh, S. F., Wada, S., Rowe, G. C., Liu, L., Chan, M. C., Rhee, J., Hoshino, A., Kim, B., Ibrahim, A., Baca, L. G., Kim, E., Ghosh, C. C., Parikh, S. M., Jiang, A., Chu, Q., Forman, D. E., Lecker, S. H., Krishnaiah, S., Rabinowitz, J. D., Weljie, A. M., Baur, J. A., Kasper, D. L. and Arany, Z. (2016) A branched-chain amino acid metabolite drives vascular fatty acid transport and causes insulin resistance. *Nat. Med.* **22**, 421-426.
Kang, W. J., Song, E. H., Park, J. Y., Park, Y. J., Cho, A. and Song, H. T. (2015) (18)F-fluoride PET imaging in a nude rat model of bone metastasis from breast cancer: comparison with (18)F-FDG and bioluminescence imaging. *Nucl. Med. Biol.* **42**, 728-733.
Kao, C. Y., Hoffman, E. A., Beck, K. C., Bellamkonda, R. V. and Annapragada, A. V. (2003) Long-residence-time nano-scale liposomal iohexol for X-ray-based blood pool imaging. *Acad. Radiol.* **10**, 475-483.
Karathanasis, E., Chan, L., Karumbaiah, L., McNeeley, K., D'Orsi, C. J., Annapragada, A. V., Sechopoulos, I. and Bellamkonda, R. V. (2009) Tumor vascular permeability to a nanoprobe correlates to tumor-specific expression levels of angiogenic markers. *PLoS ONE* **4**, e5843.
Keshari, K. R., Sriram, R., Van Criekinge, M., Wilson, D. M., Wang, Z. J., Vigneron, D. B., Peehl, D. M. and Kurhanewicz, J. (2013) Metabolic reprogramming and validation of hyperpolarized 13C lactate as a prostate cancer biomarker using a human prostate tissue slice culture bioreactor. *Prostate* **73**, 1171-1181.
Keshari, K. R. and Wilson, D. M. (2014) Chemistry and biochemistry of 13C hyperpolarized magnetic resonance using dynamic nuclear polarization. *Chem. Soc. Rev.* **43**, 1627-1659.
Kim, J. B., Urban, K., Cochran, E., Lee, S., Ang, A., Rice, B., Bata, A., Campbell, K., Coffee, R., Gorodinsky, A., Lu, Z., Zhou, H., Kishimoto, T. K. and Lassota, P. (2010) Non-invasive detection of a small number of bioluminescent cancer cells *in vivo*. *PLoS ONE* **5**, e9364.
Kim, S., Chung, J. K., Im, S. H., Jeong, J. M., Lee, D. S., Kim, D. G., Jung, H. W. and Lee, M. C. (2005) 11C-methionine PET as a prognostic marker in patients with glioma: comparison with 18F-FDG PET. *Eur. J. Nucl. Med. Mol. Imaging* **32**, 52-59.
Kimmich, G. A., Randles, J. and Brand, J. S. (1975) Assay of picomole amounts of ATP, ADP, and AMP using the luciferase enzyme system. *Anal. Biochem.* **69**, 187-206.
Koppenol, W. H., Bounds, P. L. and Dang, C. V. (2011) Otto Warburg's contributions to current concepts of cancer metabolism. *Nat. Rev. Cancer* **11**, 325-337.
Kubo, T., Ohno, Y., Takenaka, D., Nishino, M., Gautam, S., Sugimura, K., Kauczor, H. U., Hatabu, H. and iLEAD study group (2016) Standard-dose vs. low-dose CT protocols in the evaluation of localized lung lesions: capability for lesion characterization-iLEAD study. *Eur. J. Radiol. Open* **3**, 67-73.
Kurhanewicz, J. and Vigneron, D. B. (2008) Advances in MR spectroscopy of the prostate. *Magn. Reson. Imaging Clin. N. Am.* **16**, 697-710, ix-x.
Laing, R. E., Walter, M. A., Campbell, D. O., Herschman, H. R., Satyamurthy, N., Phelps, M. E., Czernin, J., Witte, O. N. and Radu, C. G. (2009) Noninvasive prediction of tumor responses to gemcitabine using positron emission tomography. *Proc. Natl. Acad. Sci. U.S.A.* **106**, 2847-2852.
Landau, M. J., Gould, D. J. and Patel, K. M. (2016) Advances in fluorescent-image guided surgery. *Ann. Transl. Med.* **4**, 392.
Lazari, M., Quinn, K. M., Claggett, S. B., Collins, J., Shah, G. J., Herman, H. E., Maraglia, B., Phelps, M. E., Moore, M. D. and van Dam, R. M. (2013) ELIXYS - a fully automated, three-reactor high-pressure radiosynthesizer for development and routine production of diverse PET tracers. *EJNMMI Res.* **3**, 52.
Le, T. M., Poddar, S., Capri, J. R., Abt, E. R., Kim, W., Wei, L., Uong, N. T., Cheng, C. M., Braas, D., Nikanjam, M., Rix, P., Merkurjev, D., Zaretsky, J., Kornblum, H. I., Ribas, A., Herschman, H. R., Whitelegge, J., Faull, K. F., Donahue, T. R., Czernin, J. and Radu, C. G. (2017) ATR inhibition facilitates targeting of leukemia dependence on convergent nucleotide biosynthetic pathways. *Nat. Commun.* **8**, 241.
Lee, J. T., Campbell, D. O., Satyamurthy, N., Czernin, J. and Radu, C. G. (2012) Stratification of nucleoside analog chemotherapy using 1-(2'-deoxy-2'-18F-fluoro-beta-D-arabinofuranosyl)cytosine and 1-(2'-deoxy-2'-18F-fluoro-beta-L-arabinofuranosyl)-5-methylcytosine PET. *J. Nucl. Med.* **53**, 275-280.
Lieberman, B. P., Ploessl, K., Wang, L., Qu, W., Zha, Z., Wise, D. R., Chodosh, L. A., Belka, G., Thompson, C. B. and Kung, H. F. (2011) PET imaging of glutaminolysis in tumors by 18F-(2S,4R)4-fluoroglutamine. *J. Nucl. Med.* **52**, 1947-1955.
Logan, A., Pell, V. R., Shaffer, K. J., Evans, C., Stanley, N. J., Robb, E. L., Prime, T. A., Chouchani, E. T., Cocheme, H. M., Fearnley, I. M., Vidoni, S., James, A. M., Porteous, C. M., Partridge, L., Krieg, T., Smith, R. A. and Murphy, M. P. (2016) Assessing the mitochondrial membrane potential in cells and *in vivo* using targeted click chemistry and mass spectrometry. *Cell Metab.* **23**, 379-385.
Lynes, M. D., Leiria, L. O., Lundh, M., Bartelt, A., Shamsi, F., Huang, T. L., Takahashi, H., Hirshman, M. F., Schlein, C., Lee, A., Baer, L. A., May, F. J., Gao, F., Narain, N. R., Chen, E. Y., Kiebish, M. A., Cypess, A. M., Bluher, M., Goodyear, L. J., Hotamisligil, G. S., Stanford, K. I. and Tseng, Y. H. (2017) The cold-induced lipokine 12,13-diHOME promotes fatty acid transport into brown adipose tissue. *Nat. Med.* **23**, 631-637.
Malone, C. F., Fromm, J. A., Maertens, O., DeRaedt, T., Ingraham, R. and Cichowski, K. (2014) Defining key signaling nodes and therapeutic biomarkers in NF1-mutant cancers. *Cancer Discov.* **4**, 1062-1073.
Mashimo, T., Pichumani, K., Vemireddy, V., Hatanpaa, K. J., Singh, D. K., Sirasanagandla, S., Nannepaga, S., Piccirillo, S. G., Kovacs, Z., Foong, C., Huang, Z., Barnett, S., Mickey, B. E., DeBerardinis, R. J., Tu, B. P., Maher, E. A. and Bachoo, R. M. (2014) Acetate is a bioenergetic substrate for human glioblastoma and brain metastases. *Cell* **159**, 1603-1614.
Mayer, I. A., Abramson, V. G., Isakoff, S. J., Forero, A., Balko, J. M., Kuba, M. G., Sanders, M. E., Yap, J. T., Van den Abbeele, A. D., Li, Y., Cantley, L. C., Winer, E. and Arteaga, C. L. (2014) Stand up to cancer phase Ib study of pan-phosphoinositide-3-kinase inhibitor buparlisib with letrozole in estrogen receptor-positive/human epidermal growth factor receptor 2-negative metastatic breast cancer. *J. Clin. Oncol.* **32**, 1202-1209.
Mayers, J. R., Torrence, M. E., Danai, L. V., Papagiannakopoulos, T., Davidson, S. M., Bauer, M. R., Lau, A. N., Ji, B. W., Dixit, P. D., Hosios, A. M., Muir, A., Chin, C. R., Freinkman, E., Jacks, T., Wolpin, B. M., Vitkup, D. and Vander Heiden, M. G. (2016) Tissue of origin dictates branched-chain amino acid metabolism in mutant Kras-driven cancers. *Science* **353**, 1161-1165.
Minn, H., Lapela, M., Klemi, P. J., Grenman, R., Leskinen, S., Lindholm, P., Bergman, J., Eronen, E., Haaparanta, M. and Joensuu, H. (1997) Prediction of survival with fluorine-18-fluoro-deoxyglucose and PET in head and neck cancer. *J. Nucl. Med.* **38**, 1907-1911.
Momcilovic, M., Bailey, S. T., Lee, J. T., Fishbein, M. C., Magyar, C., Braas, D., Graeber, T., Jackson, N. J., Czernin, J., Emberley, E., Gross, M., Janes, J., Mackinnon, A., Pan, A., Rodriguez, M., Works, M., Zhang, W., Parlati, F., Demo, S., Garon, E., Krysan, K., Walser, T. C., Dubinett, S. M., Sadeghi, S., Christofk, H. R. and Shackelford, D. B. (2017) Targeted inhibition of EGFR and glutaminase induces metabolic crisis in EGFR mutant lung cancer. *Cell Rep.* **18**, 601-610.

Momcilovic, M., McMickle, R., Abt, E., Seki, A., Simko, S. A., Magyar, C., Stout, D. B., Fishbein, M. C., Walser, T. C., Dubinett, S. M. and Shackelford, D. B. (2015) Heightening energetic stress selectively targets LKB1-deficient non-small cell lung cancers. *Cancer Res.* **75**, 4910-4922.

Mondal, S. B., Gao, S., Zhu, N., Liang, R., Gruev, V. and Achilefu, S. (2014) Real-time fluorescence image-guided oncologic surgery. *Adv. Cancer Res.* **124**, 171-211.

Morais, R., Zinkewich-Peotti, K., Parent, M., Wang, H., Babai, F. and Zollinger, M. (1994) Tumor-forming ability in athymic nude mice of human cell lines devoid of mitochondrial DNA. *Cancer Res.* **54**, 3889-3896.

Morciano, G., Sarti, A. C., Marchi, S., Missiroli, S., Falzoni, S., Raffaghello, L., Pistoia, V., Giorgi, C., Di Virgilio, F. and Pinton, P. (2017) Use of luciferase probes to measure ATP in living cells and animals. *Nat. Protoc.* **12**, 1542-1562.

Mountford, C., Ramadan, S., Stanwell, P. and Malycha, P. (2009) Proton MRS of the breast in the clinical setting. *NMR Biomed.* **22**, 54-64.

Mukundan, S., Jr., Ghaghada, K. B., Badea, C. T., Kao, C. Y., Hedlund, L. W., Provenzale, J. M., Johnson, G. A., Chen, E., Bellamkonda, R. V. and Annapragada, A. (2006) A liposomal nanoscale contrast agent for preclinical CT in mice. *AJR Am. J. Roentgenol.* **186**, 300-307.

National Lung Screening Trial Research Team, Aberle, D. R., Adams, A. M., Berg, C. D., Black, W. C., Clapp, J. D., Fagerstrom, R. M., Gareen, I. F., Gatsonis, C., Marcus, P. M. and Sicks, J. D. (2011) Reduced lung-cancer mortality with low-dose computed tomographic screening. *N. Engl. J. Med.* **365**, 395-409.

National Lung Screening Trial Research Team, Church, T. R., Black, W. C., Aberle, D. R., Berg, C. D., Clingan, K. L., Duan, F., Fagerstrom, R. M., Gareen, I. F., Gierada, D. S., Jones, G. C., Mahon, I., Marcus, P. M., Sicks, J. D., Jain, A. and Baum, S. (2013) Results of initial low-dose computed tomographic screening for lung cancer. *N. Engl. J. Med.* **368**, 1980-1991.

Nelson, S. J., Graves, E., Pirzkall, A., Li, X., Antiniw Chan, A., Vigneron, D. B. and McKnight, T. R. (2002) *In vivo* molecular imaging for planning radiation therapy of gliomas: an application of 1H MRSI. *J. Magn. Reson. Imaging* **16**, 464-476.

Nelson, S. J., Kurhanewicz, J., Vigneron, D. B., Larson, P. E., Harzstark, A. L., Ferrone, M., van Criekinge, M., Chang, J. W., Bok, R., Park, I., Reed, G., Carvajal, L., Small, E. J., Munster, P., Weinberg, V. K., Ardenkjaer-Larsen, J. H., Chen, A. P., Hurd, R. E., Odegardstuen, L. I., Robb, F. J., Tropp, J. and Murray, J. A. (2013) Metabolic imaging of patients with prostate cancer using hyperpolarized [1-(1)(3)C]pyruvate. *Sci. Transl. Med.* **5**, 198ra108.

Nielsen, J. (2017) Systems biology of metabolism: a driver for developing personalized and precision medicine. *Cell Metab.* **25**, 572-579.

Oshida, M., Uno, K., Suzuki, M., Nagashima, T., Hashimoto, H., Yagata, H., Shishikura, T., Imazeki, K. and Nakajima, N. (1998) Predicting the prognoses of breast carcinoma patients with positron emission tomography using 2-deoxy-2-fluoro[18F]-D-glucose. *Cancer* **82**, 2227-2234.

Park, H. M., Russo, K. A., Karateev, G., Park, M., Dubikovskaya, E., Kriegsfeld, L. J. and Stahl, A. (2017) A system for *in vivo* imaging of hepatic free fatty acid uptake. *Gastroenterology* **152**, 78-81.e72.

Park, I., Bok, R., Ozawa, T., Phillips, J. J., James, C. D., Vigneron, D. B., Ronen, S. M. and Nelson, S. J. (2011) Detection of early response to temozolomide treatment in brain tumors using hyperpolarized 13C MR metabolic imaging. *J. Magn. Reson. Imaging* **33**, 1284-1290.

Pirotte, B., Goldman, S., Massager, N., David, P., Wikler, D., Vandesteene, A., Salmon, I., Brotchi, J. and Levivier, M. (2004) Comparison of 18F-FDG and 11C-methionine for PET-guided stereotactic brain biopsy of gliomas. *J. Nucl. Med.* **45**, 1293-1298.

Ploessl, K., Wang, L., Lieberman, B. P., Qu, W. and Kung, H. F. (2012) Comparative evaluation of 18F-labeled glutamic acid and glutamine as tumor metabolic imaging agents. *J. Nucl. Med.* **53**, 1616-1624.

Qu, W., Oya, S., Lieberman, B. P., Ploessl, K., Wang, L., Wise, D. R., Divgi, C. R., Chodosh, L. A., Thompson, C. B. and Kung, H. F. (2012) Preparation and characterization of L-[5-11C]-glutamine for metabolic imaging of tumors. *J. Nucl. Med.* **53**, 98-105.

Qu, W., Zha, Z., Lieberman, B. P., Mancuso, A., Stetz, M., Rizzi, R., Ploessl, K., Wise, D., Thompson, C. and Kung, H. F. (2011) Facile synthesis [5-(13)C-4-(2)H(2)]-L-glutamine for hyperpolarized MRS imaging of cancer cell metabolism. *Acad. Radiol.* **18**, 932-939.

Rabinovich, B. A., Ye, Y., Etto, T., Chen, J. Q., Levitsky, H. I., Overwijk, W. W., Cooper, L. J., Gelovani, J. and Hwu, P. (2008) Visualizing fewer than 10 mouse T cells with an enhanced firefly luciferase in immunocompetent mouse models of cancer. *Proc. Natl. Acad. Sci. U.S.A.* **105**, 14342-14346.

Racker, E. (1972) Bioenergetics and the problem of tumor growth. *Am. Sci.* **60**, 56-63.

Radu, C. G., Shu, C. J., Nair-Gill, E., Shelly, S. M., Barrio, J. R., Satyamurthy, N., Phelps, M. E. and Witte, O. N. (2008) Molecular imaging of lymphoid organs and immune activation by positron emission tomography with a new [18F]-labeled 2'-deoxycytidine analog. *Nat. Med.* **14**, 783-788.

Rajeshkumar, N. V., Dutta, P., Yabuuchi, S., de Wilde, R. F., Martinez, G. V., Le, A., Kamphorst, J. J., Rabinowitz, J. D., Jain, S. K., Hidalgo, M., Dang, C. V., Gillies, R. J. and Maitra, A. (2015) Therapeutic targeting of the warburg effect in pancreatic cancer relies on an absence of p53 function. *Cancer Res.* **75**, 3355-3364.

Rampinelli, C., Origgi, D. and Bellomi, M. (2013) Low-dose CT: technique, reading methods and image interpretation. *Cancer Imaging* **12**, 548-556.

Rodrigues, T. B., Serrao, E. M., Kennedy, B. W., Hu, D. E., Kettunen, M. I. and Brindle, K. M. (2014) Magnetic resonance imaging of tumor glycolysis using hyperpolarized 13C-labeled glucose. *Nat. Med.* **20**, 93-97.

Safran, M., Kim, W. Y., Kung, A. L., Horner, J. W., DePinho, R. A. and Kaelin, W. G., Jr. (2003) Mouse reporter strain for noninvasive bioluminescent imaging of cells that have undergone Cre-mediated recombination. *Mol. Imaging* **2**, 297-302.

Salamanca-Cardona, L., Keshari, K. R. (2015) (13)C-labeled biochemical probes for the study of cancer metabolism with dynamic nuclear polarization-enhanced magnetic resonance imaging. *Cancer Metab.* **3**, 9.

Scabini, M., Stellari, F., Cappella, P., Rizzitano, S., Texido, G. and Pesenti, E. (2011) *In vivo* imaging of early stage apoptosis by measuring real-time caspase-3/7 activation. *Apoptosis* **16**, 198-207.

Schulte, M. L., Hight, M. R., Ayers, G. D., Liu, Q., Shyr, Y., Washington, M. K. and Manning, H. C. (2017) Non-invasive glutamine PET Reflects Pharmacological Inhibition of BRAFV600E *in vivo*. *Mol. Imaging Biol.* **19**, 421-428.

Serrao, E. M., Kettunen, M. I., Rodrigues, T. B., Dzien, P., Wright, A. J., Gopinathan, A., Gallagher, F. A., Lewis, D. Y., Frese, K. K., Almeida, J., Howat, W. J., Tuveson, D. A. and Brindle, K. M. (2016) MRI with hyperpolarised [1-13C]pyruvate detects advanced pancreatic preneoplasia prior to invasive disease in a mouse model. *Gut* **65**, 465-475.

Shackelford, D. B., Abt, E., Gerken, L., Vasquez, D. S., Seki, A., Leblanc, M., Wei, L., Fishbein, M. C., Czernin, J., Mischel, P. S. and Shaw, R. J. (2013) LKB1 inactivation dictates therapeutic response of non-small cell lung cancer to the metabolism drug phenformin. *Cancer Cell* **23**, 143-158.

Shi, D., Cai, G., Peng, J., Li, D., Li, X., Xu, Y. and Cai, S. (2015) The preoperative SUVmax for (18)F-FDG uptake predicts survival in patients with colorectal cancer. *BMC Cancer* **15**, 991.

Shin, P. J., Zhu, Z., Camarda, R., Bok, R. A., Zhou, A. Y., Kurhanewicz, J., Goga, A. and Vigneron, D. B. (2017) Cancer recurrence monitoring using hyperpolarized [1-13C]pyruvate metabolic imaging in murine breast cancer model. *Magn. Reson. Imaging* **43**, 105-109.

Shiomi, S., Nishiguchi, S., Ishizu, H., Iwata, Y., Sasaki, N., Tamori, A., Habu, D., Takeda, T., Kubo, S. and Ochi, H. (2001) Usefulness of positron emission tomography with fluorine-18-fluorodeoxyglucose for predicting outcome in patients with hepatocellular carcinoma. *Am. J. Gastroenterol.* **96**, 1877-1880.

Stollfuss, J., Landvogt, N., Abenstein, M., Ziegler, S., Schwaiger, M., Senekowitsch-Schmidtke, R. and Wieder, H. (2015) Non-invasive imaging of implanted peritoneal carcinomatosis in mice using PET and bioluminescence imaging. *EJNMMI Res.* **5**, 125.

Testa, C., Pultrone, C., Manners, D. N., Schiavina, R. and Lodi, R.

(2016) Metabolic imaging in prostate cancer: where we are. *Front. Oncol.* **6**, 225.
Timm, K. N., Hartl, J., Keller, M. A., Hu, D. E., Kettunen, M. I., Rodrigues, T. B., Ralser, M. and Brindle, K. M. (2015) Hyperpolarized [U-(2) H, U-(13) C]Glucose reports on glycolytic and pentose phosphate pathway activity in EL4 tumors and glycolytic activity in yeast cells. *Magn. Reson. Med.* **74**, 1543-1547.
Tseng, J. C., Narayanan, N., Ho, G., Groves, K., Delaney, J., Bao, B., Zhang, J., Morin, J., Kossodo, S., Rajopadhye, M. and Peterson, J. D. (2017) Fluorescence imaging of bombesin and transferrin receptor expression is comparable to 18F-FDG PET in early detection of sorafenib-induced changes in tumor metabolism. *PLoS ONE* **12**, e0182689.
Vahrmeijer, A. L., Hutteman, M., van der Vorst, J. R., van de Velde, C. J. and Frangioni, J. V. (2013) Image-guided cancer surgery using near-infrared fluorescence. *Nat. Rev. Clin. Oncol.* **10**, 507-518.
Van de Bittner, G. C., Dubikovskaya, E. A., Bertozzi, C. R. and Chang, C. J. (2010) *In vivo* imaging of hydrogen peroxide production in a murine tumor model with a chemoselective bioluminescent reporter. *Proc. Natl. Acad. Sci. U.S.A.* **107**, 21316-21321.
Van Laere, K., Ceyssens, S., Van Calenbergh, F., de Groot, T., Menten, J., Flamen, P., Bormans, G. and Mortelmans, L. (2005) Direct comparison of 18F-FDG and 11C-methionine PET in suspected recurrence of glioma: sensitivity, inter-observer variability and prognostic value. *Eur. J. Nucl. Med. Mol. Imaging* **32**, 39-51.
van Oosten, M., Schafer, T., Gazendam, J. A., Ohlsen, K., Tsompanidou, E., de Goffau, M. C., Harmsen, H. J., Crane, L. M., Lim, E., Francis, K. P., Cheung, L., Olive, M., Ntziachristos, V., van Dijl, J. M. and van Dam, G. M. (2013) Real-time *in vivo* imaging of invasive- and biomaterial-associated bacterial infections using fluorescently labelled vancomycin. *Nat. Commun.* **4**, 2584.
Vander Heiden, M. G. and DeBerardinis, R. J. (2017) Understanding the intersections between metabolism and cancer biology. *Cell* **168**, 657-669.
Vavere, A. L., Kridel, S. J., Wheeler, F. B. and Lewis, J. S. (2008) 1-11C-acetate as a PET radiopharmaceutical for imaging fatty acid synthase expression in prostate cancer. *J. Nucl. Med.* **49**, 327-334.
Venneti, S., Dunphy, M. P., Zhang, H., Pitter, K. L., Zanzonico, P., Campos, C., Carlin, S. D., La Rocca, G., Lyashchenko, S., Ploessl, K., Rohle, D., Omuro, A. M., Cross, J. R., Brennan, C. W., Weber, W. A., Holland, E. C., Mellinghoff, I. K., Kung, H. F., Lewis, J. S. and Thompson, C. B. (2015) Glutamine-based PET imaging facilitates enhanced metabolic evaluation of gliomas *in vivo*. *Sci. Transl. Med.* **7**, 274ra217.
Viale, A., Pettazzoni, P., Lyssiotis, C. A., Ying, H., Sanchez, N., Marchesini, M., Carugo, A., Green, T., Seth, S., Giuliani, V., Kost-Alimova, M., Muller, F., Colla, S., Nezi, L., Genovese, G., Deem, A. K., Kapoor, A., Yao, W., Brunetto, E., Kang, Y., Yuan, M., Asara, J. M., Wang, Y. A., Heffernan, T. P., Kimmelman, A. C., Wang, H., Fleming, J. B., Cantley, L. C., DePinho, R. A. and Draetta, G. F. (2014) Oncogene ablation-resistant pancreatic cancer cells depend on mitochondrial function. *Nature* **514**, 628-632.
Warburg, O. (1956a) On respiratory impairment in cancer cells. *Science* **124**, 269-270.
Warburg, O. (1956b) On the origin of cancer cells. *Science* **123**, 309-314.
Warburg, O., Wind, F. and Negelein, E. (1927) The metabolism of tumors in the body. *J. Gen. Physiol.* **8**, 519-530.
Wehrman, T. S., von Degenfeld, G., Krutzik, P. O., Nolan, G. P. and Blau, H. M. (2006) Luminescent imaging of beta-galactosidase activity in living subjects using sequential reporter-enzyme luminescence. *Nat. Methods* **3**, 295-301.
Weinberg, F., Hamanaka, R., Wheaton, W. W., Weinberg, S., Joseph, J., Lopez, M., Kalyanaraman, B., Mutlu, G. M., Budinger, G. R. and Chandel, N. S. (2010) Mitochondrial metabolism and ROS generation are essential for Kras-mediated tumorigenicity. *Proc. Natl. Acad. Sci. U.S.A.* **107**, 8788-8793.
Weinhouse, S. (1956) On respiratory impairment in cancer cells. *Science* **124**, 267-269.
Weinhouse, S., Millington, R. H. and Wenner, C. E. (1951) Metabolism of neoplastic tissue. I. The oxidation of carbohydrate and fatty acids in transplanted tumors. *Cancer Res.* **11**, 845-850.
Wenner, C. E., Spirtes, M. A. and Weinhouse, S. (1952) Metabolism of neoplastic tissue. II. A survey of enzymes of the citric acid cycle in transplanted tumors. *Cancer Res.* **12**, 44-49.
Wibmer, A. G., Burger, I. A., Sala, E., Hricak, H., Weber, W. A. and Vargas, H. A. (2016) Molecular imaging of prostate cancer. *Radiographics* **36**, 142-159.
Witney, T. H., James, M. L., Shen, B., Chang, E., Pohling, C., Arksey, N., Hoehne, A., Shuhendler, A., Park, J. H., Bodapati, D., Weber, J., Gowrishankar, G., Rao, J., Chin, F. T. and Gambhir, S. S. (2015) PET imaging of tumor glycolysis downstream of hexokinase through noninvasive measurement of pyruvate kinase M2. *Sci. Transl. Med.* **7**, 310ra169.
Woolfenden, S., Zhu, H. and Charest, A. (2009) A Cre/LoxP conditional luciferase reporter transgenic mouse for bioluminescence monitoring of tumorigenesis. *Genesis* **47**, 659-666.
Wu, Z., Zha, Z., Li, G., Lieberman, B. P., Choi, S. R., Ploessl, K. and Kung, H. F. (2014) [(18)F](2S,4S)-4-(3-Fluoropropyl)glutamine as a tumor imaging agent. *Mol. Pharm.* **11**, 3852-3866.
Yankeelov, T. E. and Gore, J. C. (2009) Dynamic contrast enhanced magnetic resonance imaging in oncology: theory, data acquisition, analysis, and examples. *Curr. Med. Imaging Rev.* **3**, 91-107.
Yao, H., So, M. K. and Rao, J. (2007) A bioluminogenic substrate for *in vivo* imaging of beta-lactamase activity. *Angew. Chem. Int. Ed. Engl.* **46**, 7031-7034.
Ying, H., Kimmelman, A. C., Lyssiotis, C. A., Hua, S., Chu, G. C., Fletcher-Sananikone, E., Locasale, J. W., Son, J., Zhang, H., Coloff, J. L., Yan, H., Wang, W., Chen, S., Viale, A., Zheng, H., Paik, J. H., Lim, C., Guimaraes, A. R., Martin, E. S., Chang, J., Hezel, A. F., Perry, S. R., Hu, J., Gan, B., Xiao, Y., Asara, J. M., Weissleder, R., Wang, Y. A., Chin, L., Cantley, L. C. and DePinho, R. A. (2012) Oncogenic Kras maintains pancreatic tumors through regulation of anabolic glucose metabolism. *Cell* **149**, 656-670.
Yoshimoto, M., Waki, A., Yonekura, Y., Sadato, N., Murata, T., Omata, N., Takahashi, N., Welch, M. J. and Fujibayashi, Y. (2001) Characterization of acetate metabolism in tumor cells in relation to cell proliferation: acetate metabolism in tumor cells. *Nucl. Med. Biol.* **28**, 117-122.
Zhang, X., Bloch, S., Akers, W. and Achilefu, S. (2012) Near-infrared molecular probes for *in vivo* imaging. *Curr. Protoc. Cytom.* **Chapter 12**, Unit12.27.
Zhou, H., Luby-Phelps, K., Mickey, B. E., Habib, A. A., Mason, R. P. and Zhao, D. (2009) Dynamic near-infrared optical imaging of 2-deoxyglucose uptake by intracranial glioma of athymic mice. *PLoS ONE* **4**, e8051.
Zhou, R., Pantel, A. R., Li, S., Lieberman, B. P., Ploessl, K., Choi, H., Blankemeyer, E., Lee, H., Kung, H. F., Mach, R. H. and Mankoff, D. A. (2017) [18F](2S,4R)4-fluoroglutamine PET detects glutamine pool size changes in triple-negative breast cancer in response to glutaminase inhibition. *Cancer Res.* **77**, 1476-1484.